

Locating Multiple Camera Sensors and Wireless Access Points for a Generalized Indoor Positioning System

Jaime Duque Domingo,
Carlos Cerrada
and J.A. Cerrada

Departamento de Ingeniería de Software y
Sistemas Informáticos
ETSI Informática, UNED,
C/Juan del Rosal, 16. 28040 Madrid, Spain
Email: ccerrada@issi.uned.es

Enrique Valero

School of Energy, Geoscience, Infrastructure and Society,
Heriot-Watt University,
Edinburgh EH14 4AS, United Kingdom
Email: e.valero@hw.ac.uk

Abstract—This work deals with the generalization of a previously developed Indoor positioning system (IPS), for estimating the location of people, based on the combination of WiFi Positioning System (WPS) and depth maps. This generalization will allow using the system in scenarios where there are multiple rooms and several people, instead of only one room with one set of sensor devices as in the initial version. The combination of both technologies improves the efficiency of existing methods, based uniquely on wireless positioning techniques, for estimating the location of people. Users just require the use of smart-phones, besides the installation of RGB-D sensors in the sensing area. But some problems arise when multiple RGB-D sensors and access points must be located in a large area composed of several rooms. The paper exposes how the necessary devices are placed minimizing the total uncovered area. The previous developed IPS is used with this placement. Experimental results for an office space composed by nine different sized rooms are shown.

Keywords—indoor positioning; IPS; WPS; RGB-D sensors; Kinect; WiFi; fingerprint; trajectory; skeletons; depth map.

I. INTRODUCTION

IPSs are systems used to obtain the position of people or objects inside a building [1]. This work extends a previously developed method for indoor positioning inside a room [2]. That work combined two known technologies: WPS, widely used in indoor positioning, and computer vision by means of RGB-D sensors. Object recognition can be considered as a part of the core research area of artificial vision, and an important number of authors have reported methods and applications for people detection and positioning. The generalization of the previous IPS will allow obtaining the user positions in complete scenarios where there are several users. The trajectories of users will be obtained by combining the two considered information sources: the WPS trajectories and the trajectories of the skeletons of the users in the *depth map*. While the positioning of the wireless sensors does not represent any real problem, special care must be taken in the location of the depth cameras in order to minimize the total uncovered area. In fact, several Kinect v2 sensors should be used simultaneously during experiments to capture the skeletons of users evolving through different rooms. This work shows how coordinates obtained by these sensors at different rooms are transformed into a universal coordinates

system (UCS). The previous technique can be applied after this transformation to obtain users positions and trajectories. The paper is structured as follows: Section 2 explores existing solutions concerning to positioning, based on WPS, RGB-D sensors, and using both technologies in a joint manner. Section 3 is devoted to analyzing the proposed system and relating it to the previous one. Special attention is given to describe how the multiple cameras should be located in a large area as considered, and how their respective coordinate systems should be related to the universal coordinate system. Section 4 presents the layout in which the experiments were performed, and analyzes the main obtained results. Finally, the Section 5 states de conclusions of the work.

II. OVERVIEW OF RELATED WORK

WPS is founded on the *fingerprinting* technique [3]. This technique creates a map of the environment recording the *Received Signal Strength Indication* (RSSI) in each point. RSSI is a reference scale used to measure the power level of signals received from a device on a wireless network (usually WiFi or mobile telephony). This map is used to obtain the position of a user in real-time, comparing the values received from the user's portable device to those stored in the map. A recent comparison between WiFi fingerprint-based indoor positioning systems have been presented by [4]. Regarding the use of advanced techniques, authors explain how to make use of temporal or spatial signal patterns, user collaboration, and motion sensors. Also, authors discuss recent advances on reducing offline labor-intensive survey, adapting to fingerprint changes, calibrating heterogeneous devices for signal collection, and achieving energy efficiency for smart-phones. In the field of people and objects detection, other technologies based on artificial vision (e.g., RGB-D sensors) have been increasingly used. Authors in [5] develop a method to detect and identify several people that are occluded by others in a scene. In [6], authors propose a *smart-cane* for the visually impaired that, with the help of a Kinect sensor, allows locating objects. The method *Kinect Positioning System* (KPS) is analyzed in [7] aiming to obtain the user position. These positioning techniques have also been used in Robotics. The work [8] presents several *Simultaneous Localization and*

Mapping (SLAM) algorithms proposed for building maps using robots with continuous positioning. By means of SLAM, the environment is built recording the measurements RSSI in each point. Also, in this field of research, the use of distinct technologies allows improving the positioning systems. [9] analyzes how to generate a *fingerprint map* with an RGB-D sensor mounted on a robot. The combination of multiple technologies improve the efficiency of traditional WPS. The work [10] proposes an hybrid indoor positioning system where WiFi and *Global System for Mobile communication* (GSM) are combined for indoor positioning. Three positioning algorithms from the Nearest Neighbor (NN) family are used for the simulations. An architecture for improving indoor positioning, by means of the combination of WiFi and RFID, is presented by [11]. WiFi is used for coordinating the RFID readers when accessing the channel for retrieving tag identifications. This avoids, in the presence of multiple readers, the so-called reader collision problem that RFID suffers. This problem is caused by the inability for direct communication among them. In [12], a robot is located using three different systems: a laser rangefinder, a depth camera, and the RSSI values. Each system is used independently according to the zone where the robot is located. Present work tries to extend a previously developed method for indoor positioning inside a room [2], which considers a scenario as represented (see Figure 1). That work combined two known technologies: WPS, widely used in indoor positioning, and computer vision by means of RGB-D sensors. In fact, it performs its activity in a single room with a single RGB-D sensor. Object recognition can be considered as a part of the core research area of computer vision, and an important number of authors have reported methods and applications for people detection and positioning. The work [13] presents an indoor human tracking application using 2 depth-cameras.

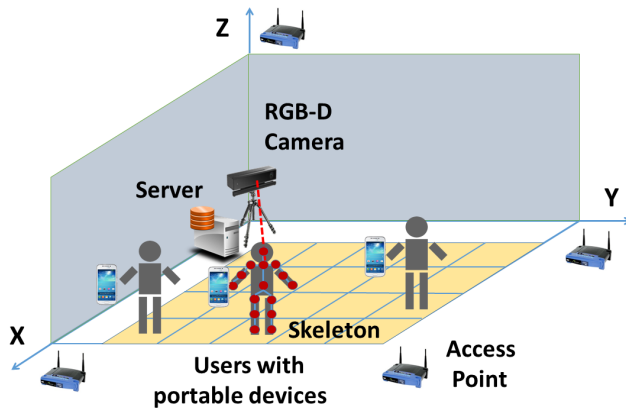


Figure 1. Scenario of the previous work

III. ANALYSIS OF THE GENERALIZED SYSTEM

The generalization of the previous IPS will allow obtaining the user identification and position in complete scenarios where there are several users. The system is valid for a complete department or company where knowing the position of each employee is useful to improve the efficiency of the business. The trajectories of users will be obtained by combining the two considered information sources: the WPS trajectories and the

trajectories of the skeletons of the users in the *depth map*. The skeletons are obtained by means of the techniques presented in [14] [15], where authors propose new algorithms to quickly and accurately predict 3D positions of body joints from depth images. Those methods form a core component of the Kinect gaming platform. The proposed system will work in a scenario composed of different rooms (see Figure 2) where there are several people, using each one a smart phone. Two or more RGB-D sensors are situated in each room for obtaining the coordinates of users by means of their skeletons. From these skeletons, neck coordinates are extracted aiming to position people in the environment. This part of the body is chosen because it is less prone to be occluded by elements in the scenario.

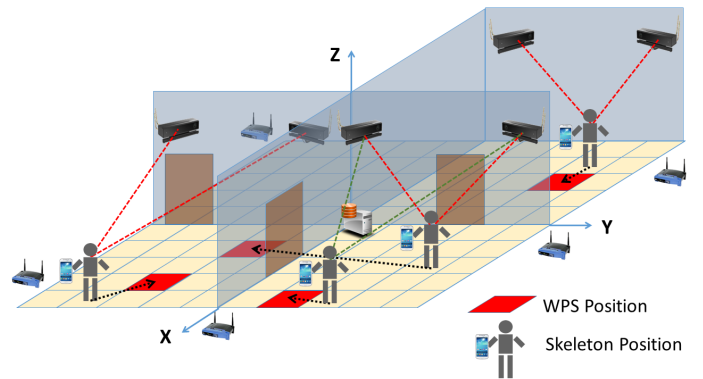


Figure 2. Scenario of the generalized system

The coordinates of the obtained skeletons represent Z_{RGB-D} axis as the distance to the RGB-D sensor while X_{RGB-D} axis is the displacement to left and right respect the sensor and Y_{RGB-D} axis represents the height (see Figure 3).

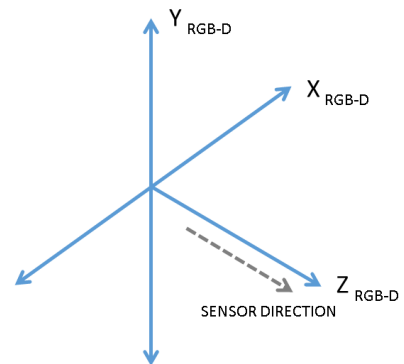


Figure 3. X_{RGB-D} , Y_{RGB-D} , and Z_{RGB-D} axis respect the RGB-D sensor direction

One unique Universal Coordinates System (UCS) is considered. For this reason, the coordinates obtained by the RGB-D sensors have to be transformed to that UCS. Because only

2D coordinates are considered in this positioning system, Y_{RGB-D} axis is ignored while Z_{RGB-D} axis corresponds to Y_{POS} axis by means of a transformation. Y_{RGB-D} axis is ignored because it represents the height of the user. In order to transform the coordinates obtained by each camera into the UCS, it is necessary to use the angle of the camera and the distance to the universal center point $P(0,0)$. Each RGB-D sensor has a different angle respect to the UCS and is situated at a different position. In this work, Kinect sensors has been used as RGB-D sensors. They have a limited angle range (see Figure 4). For this reason, they are turned to obtain a 70° angle respect the walls. It implies that is necessary to calculate the coordinates they produce into the UCS. These processes are described in the following subsections. The use of more than one RGB-D sensor allows reducing the problem of uncovered areas. Kinect sensors can obtain depth maps with a limited angle of 70° . The proposed system use two or more Kinect sensors to detect users in all positions. The parts that are not covered by a sensor, are covered by another one.

A. Position of RGB-D sensors in a room

RGB-D sensors have to be placed forming a maximum angle respect the walls. In the case of Kinect v2, the sensor is able to obtain a 70° angle. To obtain the maximum coverage, the vision line must start at the opposite corner respect the sensor. The values of X_{POS} and Y_{POS} represent the position of the sensor (see Figure 4). Kinect v2 is 25 cm wide. L represents the length of the wall.

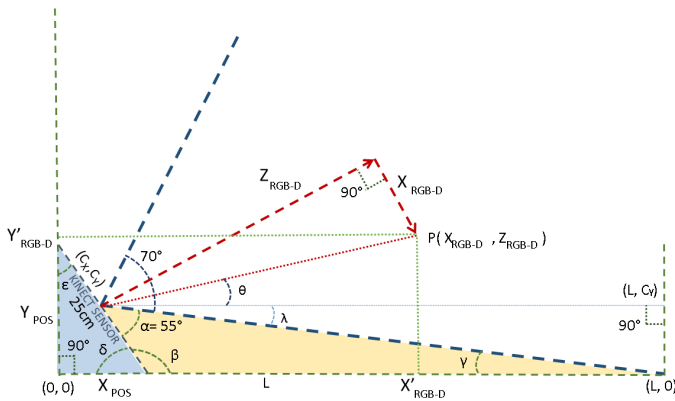


Figure 4. Position of the Kinect v2 sensor

Using the law of sines it is possible to relate both triangles and obtain the value of X_{POS} respect L . The first triangle, the one that creates the sensor with the wall represented in light blue, is solved by (1).

$$\frac{25}{\sin 90^\circ} = \frac{X_{POS}}{\sin \varepsilon} \quad (1)$$

where $90^\circ + \varepsilon + \delta = 180^\circ$. Therefore, (1) is simplified in (3).

$$\frac{25}{\sin 90^\circ} = \frac{X_{POS}}{\sin(90^\circ - \delta)} \quad (2)$$

$$X_{POS} = 25 \cdot \sin(90^\circ - \delta) \quad (3)$$

The second triangle is the one formed between the sensor and the opposite corner, represented in light yellow (see Figure 4), is solved by (4).

$$\frac{L - X_{POS}}{\sin 55^\circ} = \frac{12,5}{\sin \gamma} \quad (4)$$

where $55^\circ + \beta + \gamma = 180^\circ$ and $\beta + \delta = 180^\circ$. Therefore, $\gamma = \delta - 55^\circ$ and (4) can be modified as (6).

$$\frac{L - X_{POS}}{\sin 55^\circ} = \frac{12,5}{\sin(\delta - 55^\circ)} \quad (5)$$

$$X_{POS} = L - \frac{12,5 \cdot \sin 55^\circ}{\sin(\delta - 55^\circ)} \quad (6)$$

According to (3), it is possible to extract the value of δ (see (7))

$$\delta = 90^\circ - \arcsin \left[\frac{x}{25} \right] \quad (7)$$

Replacing δ in (6), X_{POS} is related to L (see (8)).

$$L = X_{POS} + \frac{12,5 \cdot \sin 55^\circ}{\sin(35^\circ - \arcsin \left[\frac{X_{POS}}{25} \right])} \quad (8)$$

If a Kinect v2 sensor is placed in a room with 430 cm wide ($L = 430$, X_{POS} will take the value 13,79 using (8). Y_{POS} is obtained by Pythagoras' Theorem as seen in (9).

$$X_{POS}^2 + Y_{POS}^2 = 25^2 \quad (9)$$

Therefore $Y_{POS} = 20,85$. So the Kinect sensor has to be placed at 13,79cm from the corner where the 70° angle starts, and at 20,85cm at the adjacent wall.

B. Position of RGB-D sensors respect to the UCS

The middle point of the Kinect sensor (C_X, C_Y) has to be considered for the displacements in the UCS. This point is calculated using again the law of sines (see (10)).

$$\frac{25}{\sin 90} = \frac{X_{POS}}{\sin \varepsilon} = \frac{Y_{POS}}{\sin \delta} \quad (10)$$

$$\varepsilon = \arcsin \left(\frac{X_{POS}}{25} \right) \quad (11)$$

$$\delta = \arcsin \left(\frac{Y_{POS}}{25} \right) \quad (12)$$

$$\sin(\delta) = \frac{C_Y}{12,5} \quad (13)$$

IV. EXPERIMENTATION AND RESULTS

$$\sin(\varepsilon) = \frac{C_X}{12,5} \quad (14)$$

Then, (15) is obtained and C_X and C_Y are calculated. Considering $x = 13,79\text{cm}$ and $y = 20,85\text{cm}$, then $C_X = 10,43$ and $C_Y = 6,90$.

$$\begin{cases} C_X = 12,5 \cdot \sin\left(\arcsin\left(\frac{Y_{POS}}{25}\right)\right) = \frac{Y_{POS}}{2} \\ C_Y = 12,5 \cdot \sin\left(\arcsin\left(\frac{X_{POS}}{25}\right)\right) = \frac{X_{POS}}{2} \end{cases} \quad (15)$$

Since the angle that creates the sensor with the wall is not straight, it is necessary to obtain the deviation λ . Again, this angle can be obtained using the law of sines by means of (16).

$$\frac{\sqrt{(L - C_X)^2 + (0 - C_Y)^2}}{\sin 90^\circ} = \frac{C_Y}{\sin \lambda} \quad (16)$$

Simplifying (16), (17) is obtained, where λ takes the value $1,01^\circ$ in the example.

$$\lambda = \arcsin \frac{C_Y}{\sqrt{(L - C_X)^2 + C_Y^2}} \quad (17)$$

Once λ is obtained, it is possible to obtain X'_{RGB-D} and Y'_{RGB-D} . These points represent the position of the skeleton respect the corner where the RGB-D sensor is situated. The value d_{RGB-D} is obtained by (18). It is used to simplify the rest of expressions.

$$d_{RGB-D} = \sqrt{Z_{RGB-D}^2 + X_{RGB-D}^2} \quad (18)$$

Using the law of sines, the θ angle is calculated (see (19) and (20)).

$$\frac{d_{RGB-D}}{\sin 90} = \frac{X_{RGB-D}}{\sin(35 - \lambda - \theta)} \quad (19)$$

$$\theta = 35 - \lambda - \arcsin\left(\frac{X_{RGB-D}}{d_{RGB-D}}\right) \quad (20)$$

X'_{RGB-D} and Y'_{RGB-D} are obtained using the X_{RGB-D} and Z_{RGB-D} coordinates of the skeleton obtained by the sensor (see (21)).

$$\begin{cases} X'_{RGB-D} = C_X + d_{RGB-D} \cdot \cos \theta \\ Y'_{RGB-D} = C_Y + d_{RGB-D} \cdot \sin \theta \end{cases} \quad (21)$$

When the coordinates of the RGB-D sensor respect the wall have been obtained, it is necessary to translate the coordinates to the origin of the UCS using the position of the Kinect (X_{CORNER}, Y_{CORNER}). It is also necessary to consider the side of the wall where the sensor is situated in order to select the sign of the X'_{RGB-D} and Y'_{RGB-D} coordinates. If the signs of the coordinates are positive, (22) shows how UCS coordinates are obtained.

$$\begin{cases} X_{UCS} = X_{CORNER} + X'_{RGB-D} \\ Y_{UCS} = Y_{CORNER} + Y'_{RGB-D} \end{cases} \quad (22)$$

As in our previous work [2], Kinect v2 sensors have been used as RGB-D sensors. 20 RGB-D sensor based on time-of-flight technology (ToF), Kinect v2, has been employed in these experiments. This device delivers up to 2 MPx images (1920 x 1080) at 30Hz and 0.2 MPx *depth maps* with a resolution of 512 x 424 pixels. All these Kinect are connected to a web server where data is saved and processed. The horizontal field of view of the RGB-D sensor is 70° . This system generalizes our previous work that performed the same activity in a single room with a single sensor RGB-D. The system proposed is valid for a complete department or company where the position of each employee is useful to improve the efficiency of the business. The experiments have been carried out in an office where 20 RGB-D cameras, Kinect v2, have been deployed (see Figure 5). There are 8 different rooms with a central corridor. On this corridor, 4 cameras have been deployed because of the range limitation of the sensor. Each camera is able to obtain skeletons in a 70° angle. The values of the coordinates of each skeleton have to be transformed into a universal coordination system (UCS). The central point of this UCS is situated on the left lower corner of the floor. The experiments have been developed considering the X and Y axis because all rooms are situated in the same floor.

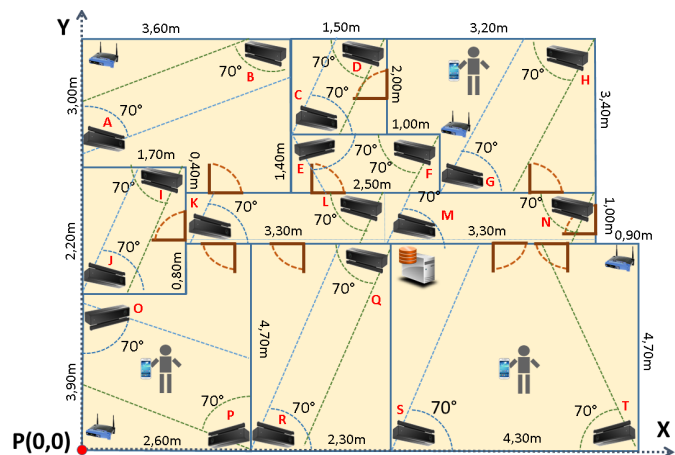


Figure 5. Scenario of the experiments

The Kinect sensors are placed on the corners using the X_{POS} and Y_{POS} displacements obtained by (8) and (9), which represent the distance between the Kinect and the corner. All these values, including the relative angle respect the wall λ obtained by (16) are shown in Tables I and II. The distance between the corners where the sensors are placed and the origin of the UCS are also shown in Table I: X_{CORNER} and Y_{CORNER} . C_X and C_Y are also taken into account to obtain the displacement of the Kinect sensor in the UCS. These values represent the necessary distance to cover the maximum angle from the wall and are calculated according to (15), as seen previously. X_{UCS} and Y_{UCS} are calculated according to the expression shown in Table II where X'_{RGB-D} and Y'_{RGB-D} are obtained using (20) and (21).

For example, the coordinates of a point obtained by the Kinect sensor E in the UCS are determined by (23).

Kinect RGB-D Camera	Corner to UCS X_{CORNER}	Corner to UCS Y_{CORNER}	Sensor to corner X_{POS}	Sensor to corner Y_{POS}	C_X	C_Y
A	0,00	6,10	0,21	0,14	0,07	0,10
B	3,60	9,10	-0,22	-0,13	0,06	0,11
C	3,60	7,10	0,13	0,21	0,06	0,11
D	5,10	9,10	-0,13	-0,21	0,06	0,11
E	3,60	7,10	0,13	-0,21	0,07	0,11
F	6,10	7,10	-0,13	-0,21	0,07	0,11
G	6,10	5,70	0,13	0,21	0,07	0,11
H	8,30	9,10	-0,14	-0,21	0,07	0,10
I	1,70	6,10	-0,13	-0,21	0,06	0,11
J	0,00	3,90	0,13	0,21	0,06	0,11
K	1,70	4,70	0,14	0,21	0,07	0,10
L	5,00	5,70	-0,14	-0,21	0,07	0,10
M	5,00	4,70	0,14	0,21	0,07	0,10
N	8,30	5,70	-0,14	-0,21	0,07	0,10
O	0,00	3,90	0,21	-0,14	0,07	0,10
P	2,60	0,00	-0,21	0,14	0,07	0,10
Q	4,90	4,70	-0,13	-0,21	0,07	0,11
R	2,60	0,00	0,13	0,21	0,07	0,11
S	4,90	0,00	0,14	0,21	0,07	0,10
T	9,20	0,00	-0,14	0,21	0,07	0,10

TABLE I. TABLE OF PARAMETERS FOR KINECT PLACEMENT (1)

Kinect RGB-D Camera	L	λ	X_{UCS}	Y_{UCS}
A	3,00	1,37°	$X_{CORNER} + Y'_{RGB-D}$	$Y_{CORNER} + X'_{RGB-D}$
B	3,40	1,10°	$X_{CORNER} - Y'_{RGB-D}$	$Y_{CORNER} - X'_{RGB-D}$
C	1,50	2,63°	$X_{CORNER} + X'_{RGB-D}$	$Y_{CORNER} + Y'_{RGB-D}$
D	1,50	2,63°	$X_{CORNER} - X'_{RGB-D}$	$Y_{CORNER} - Y'_{RGB-D}$
E	2,50	1,61°	$X_{CORNER} + X'_{RGB-D}$	$Y_{CORNER} - Y'_{RGB-D}$
F	2,50	1,61°	$X_{CORNER} - X'_{RGB-D}$	$Y_{CORNER} - Y'_{RGB-D}$
G	2,20	1,82°	$X_{CORNER} + X'_{RGB-D}$	$Y_{CORNER} + Y'_{RGB-D}$
H	3,20	1,26°	$X_{CORNER} - X'_{RGB-D}$	$Y_{CORNER} - Y'_{RGB-D}$
I	1,70	2,33°	$X_{CORNER} - X'_{RGB-D}$	$Y_{CORNER} - Y'_{RGB-D}$
J	1,70	2,33°	$X_{CORNER} + X'_{RGB-D}$	$Y_{CORNER} + Y'_{RGB-D}$
K	3,30	1,23°	$X_{CORNER} + X'_{RGB-D}$	$Y_{CORNER} + Y'_{RGB-D}$
L	3,30	1,23°	$X_{CORNER} - X'_{RGB-D}$	$Y_{CORNER} - Y'_{RGB-D}$
M	3,30	1,23°	$X_{CORNER} + X'_{RGB-D}$	$Y_{CORNER} + Y'_{RGB-D}$
N	3,30	1,23°	$X_{CORNER} - X'_{RGB-D}$	$Y_{CORNER} - Y'_{RGB-D}$
O	3,90	1,04°	$X_{CORNER} + Y'_{RGB-D}$	$Y_{CORNER} - X'_{RGB-D}$
P	4,70	0,87°	$X_{CORNER} - Y'_{RGB-D}$	$Y_{CORNER} + X'_{RGB-D}$
Q	2,30	1,74°	$X_{CORNER} - X'_{RGB-D}$	$Y_{CORNER} - Y'_{RGB-D}$
R	2,30	1,74°	$X_{CORNER} + X'_{RGB-D}$	$Y_{CORNER} + Y'_{RGB-D}$
S	4,30	0,94°	$X_{CORNER} + X'_{RGB-D}$	$Y_{CORNER} + Y'_{RGB-D}$
T	4,30	0,94°	$X_{CORNER} - X'_{RGB-D}$	$Y_{CORNER} + Y'_{RGB-D}$

TABLE II. TABLE OF PARAMETERS FOR KINECT PLACEMENT (2)

$$\begin{cases} X_{E,UCS} = 3,60 + X'_{E,RGB-D} \\ Y_{E,UCS} = 7,10 - Y'_{E,RGB-D} \end{cases} \quad (23)$$

where $X'_{E,RGB-D}$ and $Y'_{E,RGB-D}$ are obtained by (24).

$$\begin{cases} X'_{E,RGB-D} = 0,07 + d_{E,RGB-D} \cdot \cos \theta \\ Y'_{E,RGB-D} = 0,11 + d_{E,RGB-D} \cdot \sin \theta \end{cases} \quad (24)$$

$d_{E,RGB-D}$ and θ are calculated with (25) and (26) respectively.

$$d_{E,RGB-D} = \sqrt{Z_{E,RGB-D}^2 + X_{E,RGB-D}^2} \quad (25)$$

$$\theta = 35 - 1,61 - \arcsin\left(\frac{X_{E,RGB-D}}{d_{E,RGB-D}}\right) \quad (26)$$

Finally, (27) shows how to obtain $X_{E,UCS}$ and $Y_{E,UCS}$ coordinates from the Kinect coordinates $X_{E,RGB-D}$ and $Y_{E,RGB-D}$.

$$\begin{cases} X_{E,UCS} = 3,67 + d_{E,RGB-D} \\ \cdot \cos\left(33,39 - \arcsin\left(\frac{X_{E,RGB-D}}{d_{E,RGB-D}}\right)\right) \\ Y_{E,UCS} = 6,99 - d_{E,RGB-D} \\ \cdot \sin\left(33,39 - \arcsin\left(\frac{X_{E,RGB-D}}{d_{E,RGB-D}}\right)\right) \end{cases} \quad (27)$$

The developed experiments have shown an important advance in terms of indoor positioning. The system is able to locate more than 10 people with a success over 95% (see Figure 6) in a scenario with multiple rooms. The scenario has a size of 80 square meters and 8 rooms. The users have followed different trajectories.

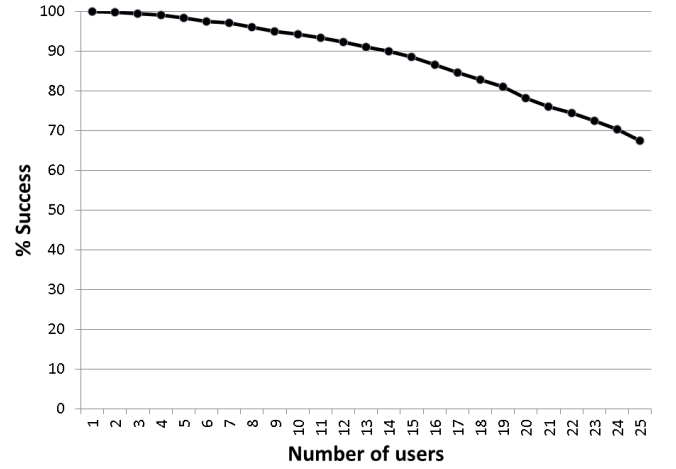


Figure 6. Results for a different number of users

V. CONCLUSIONS

This work presents an extended method for indoor positioning based on a previously developed algorithm, which worked exclusively with one room. This new method allows obtaining indoor positioning inside a complete floor or building. Twenty RGB-D sensor have been used to obtain the *depth maps* and, subsequently, the skeletons. The combination of wireless networks with skeletons is a simple and economical method to increase the performance of WPS in interiors. The generalization of the previous IPS allows obtaining the user positions in large areas where there are several users. The trajectories of users can be obtained by combining the two considered information sources: the WPS trajectories and the trajectories of the skeletons of the users in the *depth map*. Although the positioning of the wireless sensors in the complete scenario does not represent a real problem, special attention has been paid to the location of the depth cameras. The purpose has been avoiding blind areas, minimizing the total uncovered area. The work has also shown how coordinates obtained from the depth cameras at different rooms are transformed into a universal coordinates system (UCS). At this point, the previous technique can be applied to obtain users positions and

trajectories. The position of the sensors is followed by [16], where authors consider the use of this system to obtain the positions of the users in a museum. That work is an approach to enrich the indoor user experience.

CONFLICTS OF INTEREST

The authors declare that there is no conflict of interest regarding the publication of this manuscript.

ACKNOWLEDGMENTS

This work has been developed with the help of the research projects DPI2013-44776-R and DPI2016-77677-P of MICINN. It also belongs to the activities carried out within the framework of the research network CAM RoboCity2030 S2013/MIT-2748 of Comunidad de Madrid

REFERENCES

- [1] G. Deak, K. Curran, and J. Condell, "A survey of active and passive indoor localisation systems," *Computer Communications*, vol. 35, no. 16, 2012, pp. 1939–1954.
- [2] J. Duque Domingo, C. Cerrada, E. Valero, and J. Cerrada, "Indoor positioning system using depth maps and wireless networks," *Journal of Sensors*, vol. 2016, 2016.
- [3] W. Liu, Y. Chen, Y. Xiong, L. Sun, and H. Zhu, "Optimization of sampling cell size for fingerprint positioning," *International Journal of Distributed Sensor Networks*, vol. 2014, 2014.
- [4] S. He and S.-H. G. Chan, "Wi-fi fingerprint-based indoor positioning: Recent advances and comparisons," *IEEE Communications Surveys & Tutorials*, vol. 18, no. 1, 2016, pp. 466–490.
- [5] G. Ye, Y. Liu, Y. Deng, N. Hasler, X. Ji, Q. Dai, and C. Theobalt, "Free-viewpoint video of human actors using multiple handheld kinects," *Cybernetics, IEEE Transactions on*, vol. 43, no. 5, 2013, pp. 1370–1382.
- [6] H. Takizawa, S. Yamaguchi, M. Aoyagi, N. Ezaki, and S. Mizuno, "Kinect cane: object recognition aids for the visually impaired," in *Human System Interaction (HSI), 2013 The 6th International Conference on*. IEEE, 2013, pp. 473–478.
- [7] Y. Nakano, K. Izutsu, K. Tajitsu, K. Kai, and T. Tatsumi, "Kinect positioning system (kps) and its potential applications," in *International Conference on Indoor Positioning and Indoor Navigation*, vol. 13, 2012, p. 15th.
- [8] C. K. Schindhelm, "Evaluating slam approaches for microsoft kinect," in *Proc. 2011 The Eighth International Conference on Wireless and Mobile Communications (ICWMC 2012), Venice, 2012*, pp. 402–407.
- [9] P. Mirowski, R. Palaniappan, and T. K. Ho, "Depth camera slam on a low-cost wifi mapping robot," in *Technologies for Practical Robot Applications (TePRA), 2012 IEEE International Conference on*. IEEE, 2012, pp. 1–6.
- [10] J. Machaj and P. Brida, "Impact of optimization algorithms on hybrid indoor positioning based on gsm and wi-fi signals," *Concurrency and Computation: Practice and Experience*, 2016.
- [11] A. Papapostolou and H. Chaouchi, "Integrating rfid and wlan for indoor positioning and ip movement detection," *Wireless Networks*, vol. 18, no. 7, 2012, pp. 861–879.
- [12] J. Biswas and M. Veloso, "Multi-sensor mobile robot localization for diverse environments," in *RoboCup 2013: Robot World Cup XVII*. Springer, 2014, pp. 468–479.
- [13] M. R. U. Saputra, W. Widyawan, G. D. Putra, and P. I. Santosa, "Indoor human tracking application using multiple depth-cameras," in *Advanced Computer Science and Information Systems (ICACSIS), 2012 International Conference on*. IEEE, 2012, pp. 307–312.
- [14] J. Shotton, T. Sharp, A. Kipman, A. Fitzgibbon, M. Finocchio, A. Blake, M. Cook, and R. Moore, "Real-time human pose recognition in parts from single depth images," *Communications of the ACM*, vol. 56, no. 1, 2013, pp. 116–124.
- [15] A. Barmpoutis, "Tensor body: Real-time reconstruction of the human body and avatar synthesis from rgb-d," *Cybernetics, IEEE Transactions on*, vol. 43, no. 5, 2013, pp. 1347–1356.
- [16] J. Duque-Domingo, P. J. Herrera, E. Valero, and C. Cerrada, "Deciphering egyptian hieroglyphs: Towards a new strategy for navigation in museums," *Sensors*, vol. 17, no. 3, 2017, p. 589.